Facile Fabrication of Tough SiC Inverse Opal Photonic Crystals

Jinming Zhou,[†,‡] Huiling Li,[†] Li Ye,[†] Jian Liu,[†,‡] Jingxia Wang,*[,†] Tong Zhao,[†] Lei Jiang,[†] and Yanlin Song*[,†]

Beijing National Laboratory for Molecular Sciences (BNLMS), Laboratory of New Materials, Key Laboratory of Organic Solids, Laboratory of Advanced Polymer Materials, Institute of Chemistry, Chinese Academy of Sciences, Beijing 100190, P. R. China, and Graduate University of Chinese Academy of Sciences, Beijing 100049, P. R. China

Received: September 18, 2010; Revised Manuscript Received: November 11, 2010

In this work, large-scale SiC inverse opal photonic crystals (PCs) with stopbands covering the entire UV−vis−NIR range have been first fabricated via sacrificial template method. The resultant PCs show superhydrophilicity, tough solvent resistance and high mechanical strength, whose structure color keeps almost constant after immersed in organic solvents or strong acid/base solutions for longer than 120 h. The hardness and Young's modulus of the achieved PCs can reach 0.56 and 25 GPa respectively, which is the highest value for inverse opal PCs. Moreover, enhanced photoluminescence of SiC can be achieved with optimized PC stopband. This large-scale fabrication of SiC PCs with good optical property will greatly extend the practical applications of PCs in harsh environments.

Introduction

Nowadays, photonic crystals (PCs) have aroused considerable interest due to their special light manipulating properties and wide applications in optics, such as high efficiency light emitting diodes,[1] microcavity lasers,[2] and fluorescence enhancement.[3] Among them, inverse opal PCs are especially important because their photonic bandgap can be enhanced by the high refraction index contrast. Thus, many efforts have focused on the fabrication of inverse opal PCs from various materials such as silicon,[4] carbon,[5] metals,[6] oxide ceramics[7] and polymers.[8] However, there are some application limits for current PC materials. For example, carbon and polymers can not be utilized at high temperature in air. Silicon, metals, and oxide ceramics show low corrosion resistance or poor mechanical strength.[9] To meet the practical application requirements, more advanced inverse opal matrix with higher thermal stability, better corrosion resistance and mechanical stability is expected. Herein, SiC inverse opal PCs with tough mechanical strength and solvent resistance, are fabricated, which will greatly extend the practical applications of PCs in harsh environments.

SiC is a promising material for application in extreme environments due to its excellent thermal stability, good chemical inertness and high hardness/strength.[10] In this aspect, ordered SiC porous structures have attracted much research interest because of their potential applications in ultrahigh temperature catalysis, tough electronic, and photonic devices.[11] For instance, Zhao and Shi et al. fabricated well-ordered mesoporous and hierarchically macro-mesoporous SiC.[11a,b] Kim et al. utilized these SiC porous materials as a high-temperature catalyst support for fuel reforming.[11c−f] It is expected that endowing the ordered porous SiC structures with light manipulation properties will greatly broaden their promising applications in various optic devices. However, few work has reported on the fabrication of SiC PCs with good optic properties, which can be attributed to a lack of proper SiC precursor polymer or poor film integrity resulted from the acid etching process for removing template[11c−f] or byproduct.[11b] In this article, we demonstrated a facile fabrication of tough SiC inverse opal PCs with large area and good optical properties via sacrificial template method. This successful fabrication was mainly attributed to the suitable selection of SiC preceramic precursor of silylene−acetylene. The low curing temperature (60 °C) and good solubility of the preceramic polymer are favorable for the use of opal template assembled from highly monodispersed latex spheres of poly(styrene−methyl methacrylate−acrylic acid) (p(St−MMA−AA)). The octane solution of the preceramic polymer can fully wet and spread in the opal template, facilitating their homogeneous infiltration. Besides, the opal template could be easily removed from calcination process. All of these contribute to the achievement of large-area SiC PCs with high film integrity, good optic properties, excellent solvent resistance and high mechanical strength. The photoluminescence (PL) of the SiC can be effectively improved by 6.3 times with the optimized stopband. This facile fabrication of SiC PCs will greatly extend PCs' applications in harsh atmospheres.

Experimental Section

Fabrication of Silylene−Acetylene Preceramic Polymer and p(St−MMA−AA) Opal Templates. Silylene−acetylene preceramic polymer[12] and monodispersed latex spheres of p(St−MMA−AA)[13] were synthesized via our previous method. The resultant latex spheres were used directly without purification. The opal templates were fabricated on quartz substrates by a vertical deposition method. After drying, the opal templates were sintered at 85 °C for 30 min to increase the stability of the films.

Fabrication of SiC Inverse Opal PCs. SiC inverse opal PCs were fabricated through sacrificial template method. First, silylene−acetylene preceramic polymer was dissolved in octane with the concentration of 0.5 gmL^{-1}. Then chloro platinic acid catalyst in tetrahydrofuran was added into the preceramic polymer solution with a concentration of 5×10^{-4} gmL^{-1}.

* To whom correspondence should be addressed. E-mail: ylsong@iccas.ac.cn (Y.S.), wangzhang@iccas.ac.cn (J.W.).
† Beijing National Laboratory for Molecular Sciences (BNLMS).
‡ Graduate University of Chinese Academy of Sciences.

10.1021/jp108928g
Published on Web 12/02/2010

SCHEME 1: Scheme Illustration of the Fabrication Process of SiC Inverse Opal PCs; the Inserted Chemical Structure is Silylene−Acetylene Pre-ceramic Polymer

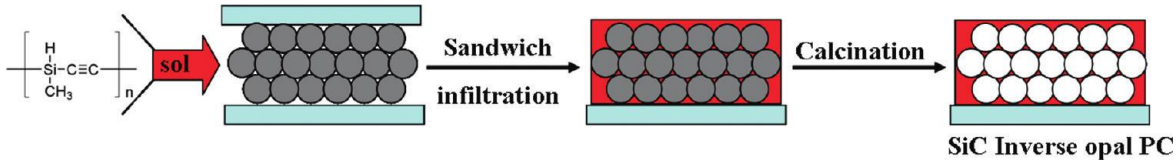

Subsequently, the as-prepared silylene−acetylene preceramic solution was infiltrated into the interstices of the as-prepared opal template using sandwich method in a glovebox (Mikrouna, China) with Ar atmosphere. The infiltration was repeated twice and the infiltrated film was cured at 60 °C for half an hour. Then, the cured film was sintered at 600−1200 °C in a tubular furnace (Nabertherm) within Ar atmosphere. In the calcination process, the preceramic polymer was pyrolyzed into SiC. At the same time, the template was removed and SiC inverse opal PC was achieved.

The control sample for PL enhancement tests was prepared by drop coating the preceramic polymer solution onto a clean quartz substrate and subsequently sintered at 600−1200 °C in a tubular furnace within Ar atmosphere.

Characterization. SEM images were taken by Hitachi FE-S4800 and JEOL JSM-6700 microscopy (Japan). The contact angle was measured on Dataphysics (Germany) OCA20 contact-angle system at ambient temperature. High-resolution TEM (HRTEM) image was obtained on a JEOL JEM-2100 TEM (Japan) operating at 200 kV. Samples for TEM measurement were obtained by scratching them off the substrate and dispersing in ethanol. Carbon coated copper grids were used as the sample holder. XRD patterns were collected on a Rigaku D/MAX 2500 X-ray diffractometer using a high-power Cu Kα radiation. ^{29}Si magnetic angle spinning NMR (MAS NMR) spectrum was collected on Digital Nuclear Magnetic Resonance Spetrometer Avance III 400 MHz. An Ocean Optic (USA) fiber optic UV−vis−NIR spectrometer was used for the evaluation of the optical characteristics of the SiC PCs. All reflectance spectra were measured at normal incidence to the (111) planes. Photographs were taken by a digital camera (Canon EOX 450D). Both hardness and Young's modulus were measured using a nanoindentation continuous stiffness method (Nano Indenter XP, MTS). Single spectrum and confocal modes of a Witec-Alpha scanning near-field optical microscope (equipped with a liquid-nitrogen cooled (−56 °C) CCD camera detector) were used for PL measurements with a 442 nm excitation. The femtosecond laser was passed through a beam expander and an objective to be focused on the PCs with a spot size of ca. 2 μm. All spectra were recorded normal to the (111) planes of the PCs.

Results and Discussion

1. Fabrication and Characterization of SiC Inverse Opal PCs. SiC inverse opal PCs are fabricated via sacrificial template method as illustrated in Scheme 1. First, an octane solution of silylene-acetylene preceramic polymer is infiltrated into the opal template in Ar atmosphere using the sandwich method. The infiltrated film is subsequently cured at 60 °C for cross-linking of the preceramic polymer. Second, the cured film is sintered at 600−1200 °C within Ar atmosphere for 2 h. During the calcination process, the silylene−acetylene is pyrolyzed into SiC. At the same time, the opal template is removed and SiC inverse opal PC is obtained.

The opal template is prepared through vertical deposition method by using latex suspension of monodisperse

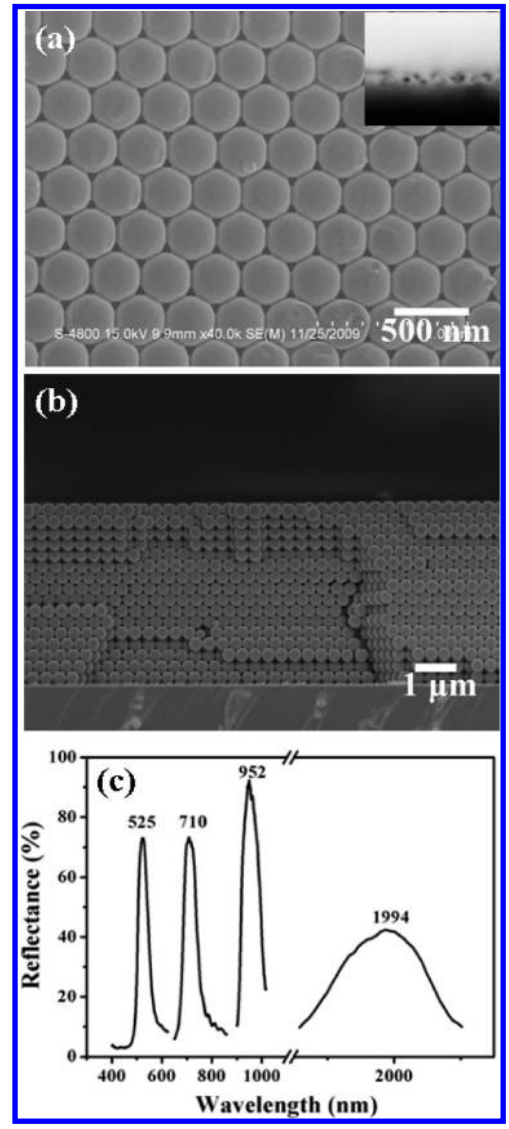

Figure 1. (a) Top view and (b) cross-section view SEM images of the opal template assembled from monodispersed p(St−MMA−AA) spheres with diameter of ca. 318 nm. (c) Reflectance spectra of the opal templates assembled from monodispersed p(St−MMA−AA) spheres with diameters ca. 190, 318, 412, and 710 nm respectively, inserted numbers indicate the stopband positions (nm) of PC templates. The insert in (a) is the contact angle (nearly 0°) of the octane solution of the preceramic polymer on the template.

p(St−MMA−AA)[13] with diameters of ca. 190, 318, 412, and 710 nm, respectively. Parts a and b of Figure 1 show typical SEM images of the opal template with latex diameter of ca. 318 nm. Clearly, the latex spheres are arranged in a well-ordered face-centered-cubic close-packed structure. The highly ordered periodicity of the opal template results in good optical properties in part c of Figure 1, which contributes to the achievement of well-ordered SiC inverse opal PCs. It should be mentioned that the spectrum intensity is relatively low for PC assembled from

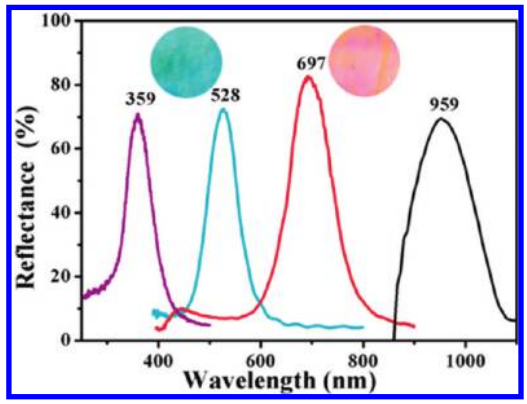

Figure 2. Reflectance spectra of as-prepared SiC inverse opal PCs obtained at 600 °C. The inserted numbers indicate the stopband positions (nm). The value from left to right is corresponding to the opal templates assembled from latex spheres with diameters of ca. 190, 318, 412, and 710 nm, respectively. The inserted digital photographs are the samples with stopbands at 528 and 697 nm, respectively.

latex spheres with diameter of *ca.* 710 nm, which may be due to the difficulty in self-assembly for large latex spheres.

Highly ordered SiC inverse opal PCs are obtained after infiltrating SiC precursor into the opal templates and subsequent curing and calcination. The optical property of as-prepared SiC PC is characterized in Figure 2. Intense and narrow reflectance peaks are recorded, which verifies the good optical property of as-prepared PCs. Comparing with the reflectance spectra of the corresponding opal templates in part c of Figure 1, large blue shifts occur to the stopband positions of SiC PCs. These shifts could be attributed to the decrease of the average refraction index and the shrinkages of the macropores during the calcination procedure.[14] Otherwise, there is a little widening of the spectra for the inverse opal PCs compared with that of the opal template, which may be due to the scattering effects of cracks formed in the calcination process.[15] However, no obvious reflectance intensity fall and even a clear increase in the infrared region is observed, which suggests the structure of the opal template is well maintained in the SiC inverse opal replica. The inserted photos in Figure 2 demonstrate that the samples show iridescently green and red color, corresponding to their stopbands of 528 and 697 nm, respectively. The bright colors are due to the Bragg diffraction of the well-ordered periodicity of as-prepared SiC PCs, which can be clearly confirmed by SEM images in parts a and b of Figure 3. From the top view image of part a of Figure 3, a highly ordered SiC scaffold can be observed and air spheres are in a face-centered-cubic arrangement over the entire sample area with the close-packed (111) plane oriented parallel to the substrate. The cross-sectional SEM image in part b of Figure 3 exhibits that the air spheres are in contact with the neighboring underlayer and the thickness of as-prepared SiC inverse opal is about 4 μm. This highly ordered periodicity of SiC PCs contributes to the excellent optical property in Figure 2. It should be mentioned that the area of SiC PCs is ca. 4 cm^2 in our experiment.

This fabrication of high-quality SiC PCs is mainly attributed to the use of silylene−acetylene preceramic polymer synthesized in our lab.[12] The polymer can cross-link and solidify at 60 °C. This low solidification temperature makes it feasible to utilize the highly monodisperse p(St−MMA−AA)[13] spheres with T_g of 107 °C for opal template. The opal template can be removed in the calcination process, avoiding additional acid etching treatment,[11b−f] which ensures the achievement of large scale SiC PCs with well-ordered periodicity in Figure 3. Otherwise, the preceramic polymer is soluble in various solvents, that is tetrahydrofuran, toluene, trichloromethane, hexane, and octane. This good solubility favors the suitable selection of solvent, which is a good solvent for the preceramic polymer but a poor solvent for the polymer opal template. Meantime, the preceramic polymer solution should fully wet, spread and homogeneously infiltrate in the template. The anticipated wettability is confirmed by the nearly 0° contact angle of the precursor solution (in octane) on the opal template (insert in part a of Figure 1). Above all, the low curing temperature and good solubility of silylene−acetylene preceramic polymer enable us to use the highly monodisperse p(St−MMA−AA) spheres as template. The octane solution of preceramic polymer favors the homogeneous infiltration into the template, which contributes to the successful fabrication of SiC PCs with large area and good optical property. This facile fabrication of SiC PCs will throw a new light for the promising applications of SiC or PCs in high-performance optic devices.

To clarify the composition of the as-prepared sample, ^{29}Si MAS NMR and HRTEM are employed to characterize the product obtained at 600 °C in Figure 4. The ^{29}Si MAS NMR spectrum (part a of Figure 4) of the sample is centered at −15.9 ppm, covering a range between −30 and 10 ppm, which indicates the formation of amorphous SiC.[16] HRTEM in part b of Figure 4 shows nanoscale crystalline domains with a lattice *d* spacing of 0.25 nm, suggesting the presence of crystalline β-SiC in the resultant sample.[17]

2. Influence of Calcination Temperature on the Crystallinity and Optic properties of SiC PCs. It is well-known that increasing calcination temperature can improve the crystallinity of the samples. Here, calcination temperature produces a distinct influence on the crystallinity and optic properties of SiC PCs. There is an increase in crystallinity of the sample when further raising calcination temperature, which can be clearly observed by the XRD results in part a of Figure 5. No intense diffraction peaks can be observed when the calcination temperature is lower than 1000 °C, suggesting the formation of amorphous SiC. In contrast, intense diffraction peaks can be clearly observed for

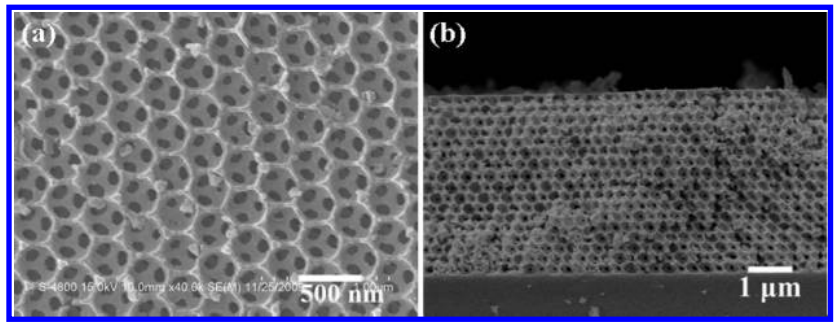

Figure 3. (a) Top view and (b) cross-sectional view SEM images of as-prepared SiC PCs obtained at 600 °C.

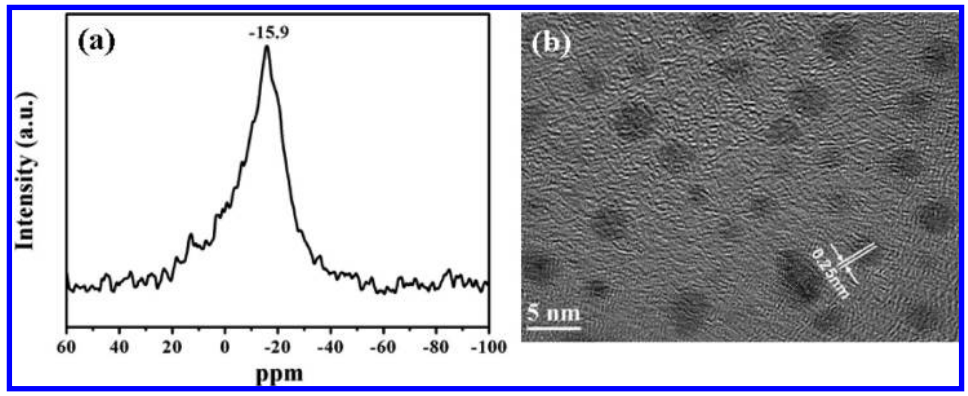

Figure 4. (a) ^{29}Si MAS NMR spectra and (b) HRTEM image of SiC sample obtained at 600 °C.

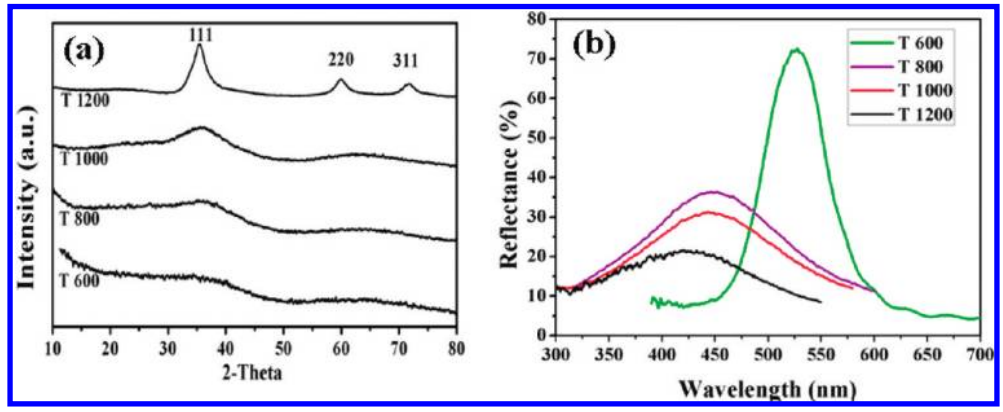

Figure 5. (a) XRD patterns and (b) reflectance spectra of SiC samples fabricated at different calcination temperatures. Inserted numbers indicate (111), (220) and (311) crystalline planes of β-SiC.

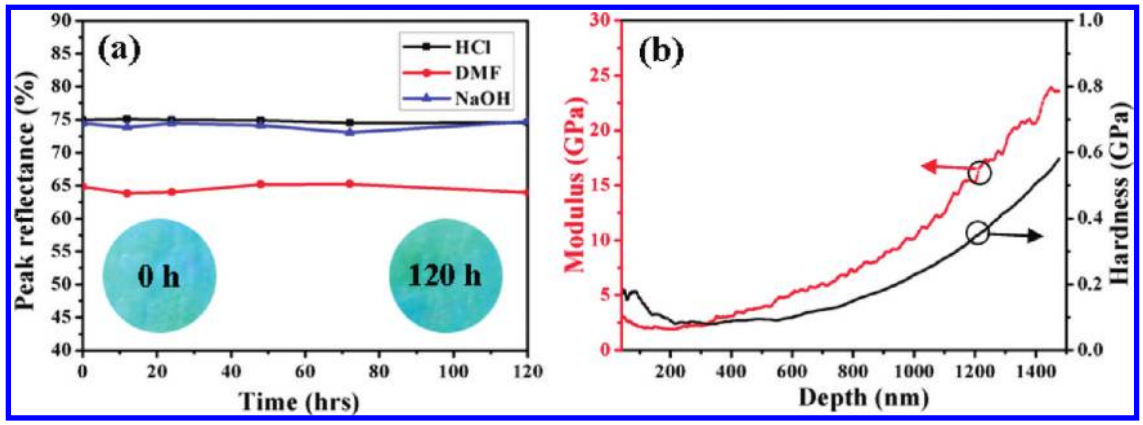

Figure 6. (a) Reflectance intensity of as-prepared SiC PCs after being immersed in DMF, concentrated HCl and aqueous NaOH solution (2M) for 0, 12, 24, 72, and 120 h. (b) Hardness and modulus curves of as-prepared SiC PCs.

the sample obtained at 1200 °C, which correspond to the (111) (220) and (311) planes of β-SiC.[18] On the other hand, the stopband positions of SiC PCs blue-shift to shorter wavelength with increasing temperatures in part b of Figure 5. In detail, an intense reflectance peak is recorded at 528 nm when calcinated at 600 °C, and the stopband positions blue-shift to 453, 449, and 428 nm respectively when the sample was calcinated at 800, 1000, and 1200 °C. This blue shift could be attributed to the decrease in the spacing between crystalline planes in the direction normal to (111) based on Bragg's diffraction law. The decrease in crystal spacing is due to the increased shrinkages ratio of the macrospores at higher calcination temperatures (Figure S1 of the Supporting Information). These shrinkages bring about structure defects and lead to lower peak intensity and broad spectra.[19] Additionally, SiC absorption in the UV region also accounts for the decline in the reflectance intensity.[20]

3. Durability and Superhydrophilicity of SiC PCs. The as-prepared SiC PCs can endure various solvents, that is ethanol, sodium hydroxide solution (2 M), concentrated hydrochloric acid, toluene, dimethyformamide, and tetrahydrofuran. No obvious decrease of the reflectance intensity is observed after the films are immersed in these solvents for 120 h in part a of Figure 6 and Figure S2 of the Supporting Information, although slight red shifts of the stopbands are recorded (Figure S2 of the Supporting Information). The red shifts are ascribed to the solvents absorption into the porous structures.[21] Otherwise, SiC PCs obtained at 600 °C show high mechanical stability in part b of Figure 6. The Young modulus and hardness of as-prepared SiC PCs are 25 and 0.56 GPa respectively, which is estimated from depth-sensing nanoindentation.[22] The value is the highest result for inverse opal PCs, which would endow the films with

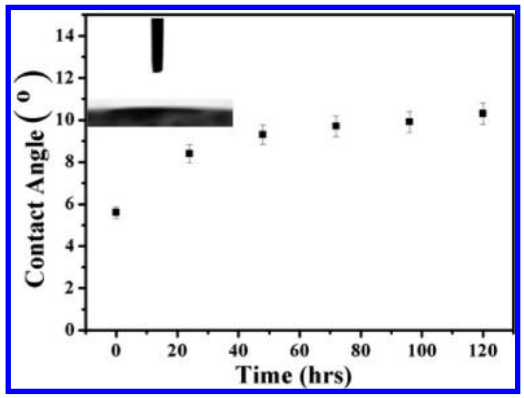

Figure 7. Changes of static contact angle versus storing time in ambient atmosphere. The insert shows a static contact angle of about 5.7°.

special application in high pressure atmosphere where common PC can not.[22]

It should be mentioned that the ordered structure of PCs not only contributes to the iridescent structural colors in Figure 2, but also endows the surface with superhydrophilicity. The measured static water contact angle is ca. 5.7° (insert in Figure 7) for the newly prepared sample and the superhydrophilicity of SiC PCs is stable for 120 h in Figure 7. The superhydrophilicity can mainly be attributed to the combined effect of the rough structure resulted from the periodic microstructure and the hydrophilicity of the SiC materials.[21b,23] In this case, water extends on the surface easily and wedges into the space between the substrate, removing the dusts off the surface.[24] This self-cleaning property (resulting from superhydrophilicity) of as-prepared SiC PCs is highly favorable for their practical applications.

4. Enhanced PL of SiC PCs. The blue-green PL of SiC[25] has promising applications in optic devices, such as displays, light emitting devices and biosensors. But the indirect bandgap nature of SiC results in its low PL intensity, which greatly restricts its optic applications. To solve this problem, single-crystal SiC was etched[25a] or spark-processed[25b] into porous structure and PL enhancement was achieved. But single-crystal SiC is costly and above-mentioned process requires special equipments. The fabrication of SiC PCs may provide a facile approach to improve its PL based on the special light manipulating properties of PC structure, which has been widely utilized to enhance the fluorescence of organic dyes based on its stopband and slow photon effect.[3,26] Because of the fact that the group velocity of photons at the PC stopband edges can be slowed down, the photons can be thereby localized in the PCs, giving rise to larger density of optical states. The interaction between photons and SiC can be enhanced.[26] As expected, the as-prepared SiC PCs can lead to a dramatic modification of light propagation and the emission properties of SiC, which produces an obvious PL enhancement based on the optical gain of PC structure,[26] as shown in Figure 8 (the detailed data are listed in Figure S4 of the Supporting Information).

The PL enhancement factors vary from 1.2 to 6.3 for SiC PCs with different stopbands (parts a and b of Figure 8). Clearly, the control sample shows a weak wide emission with a peak centered at 568 nm (part a of Figure 8, black dash line and part a of Figure S4 of the Supporting Information), which is consistent with the electron bandgap of β-SiC.[27] PL enhancements of 6.3, 5.1, and 4.5 times can be achieved with PC_{em1} ($\lambda_{stopband} = 528$ nm, whose red band edge overlaps the emission peak of bulk SiC ($\lambda_{em} = 568$ nm)), PC_{ex} ($\lambda_{stopband} = 432$ nm, whose red band edge overlaps the laser excitation ($\lambda_{ex} = 442$ nm)), and PC_{em2} ($\lambda_{stopband} = 697$ nm, whose blue band edge overlaps the emission peak of bulk SiC ($\lambda_{em} = 568$ nm)), respectively. In contrast, about 1.2 times enhancement (Figure S4e-f) is detected when the stopband overlaps nothing with the SiC emission or laser excitation for PC_{off1} ($\lambda_{stopband} = 717$ nm), PC_{off2} ($\lambda_{stopband} = 959$ nm) and PC_{off3} ($\lambda_{stopband} = 359$ nm), which indicates that only ca. 1.2 times PL enhancement is due to the porous structure when only utilizing PC structures without matching to SiC emission or laser excitation. While upmost ca. 6.3 fold PL enhancement is resulted from the combination of macroporous structure and slow photon effect of PCs. These indicates that ca. 5.3 times PL enhancement originates from the slow photon effect of PC (Table S1 of the Supporting Information), and the value is comparable to that of optical gain of quantum dots[26c] or organic dye[3e] on the surface of PCs. Compared with the reported PL enhancement (2 times for spark-processed SiC) resulted from SiC porous structure,[25b] the PL enhancement based on PC structure provides a facile and low-cost enhancement strategy for SiC, which has profound implications for SiC applications as optical devices in harsh environments.

Conclusions

Large-scale SiC inverse opal PCs with high quality have been first fabricated via sacrificial template method, with their stopbands covering the entire UV−vis−NIR range. This successful fabrication is mainly attributed to the low curing

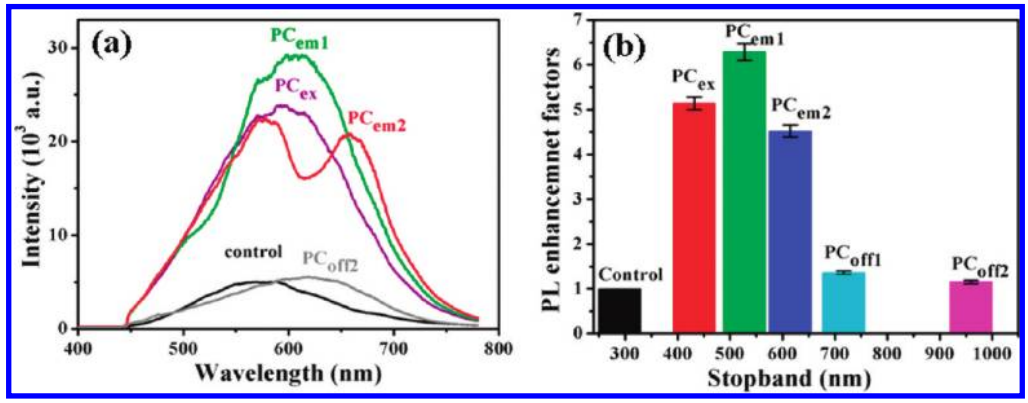

Figure 8. (a) PL spectra and (b) PL enhancement factors of SiC PCs with different stopbands. The factors are the ratios of the PL intensity of PCs to that of control sample. PC_{em1}: $\lambda_{stopband} = 528$ nm, whose red band edge overlaps the emission peak of bulk SiC ($\lambda_{em} = 568$ nm), PC_{em2}: $\lambda_{stopband} = 615$ nm, whose blue band edge overlapse the emission of bulk SiC. PC_{ex}: $\lambda_{stopband} = 432$ nm, whose red band edge overlaps the laser excitation ($\lambda_{ex} = 442$ nm). PC_{off1} ($\lambda_{stopband} = 717$ nm), $PC_{off\ 2}$ ($\lambda_{stopband} = 959$ nm) and $PC_{off\ 3}$ ($\lambda_{stopband} = 359$ nm), whose stopbands overlap nothing with SiC emission or laser excitation.

temperature and good solubility of the preceramic polymer, which is favorable for the use of opal template assembled from highly monodispersed polymer spheres. The octane solution of preceramic polymer facilitates its homogeneous infiltration into the template due to their matched wettability. The resultant SiC PCs show superhydrophilicity, excellent solvent resistance and high mechanical strength. Moreover, the PL of the SiC PCs could be improved by 6.3 times with optimized stopband. This facile fabrication of large scale SiC PCs with good optical property will greatly extend PC's applications in harsh environments and SiC's applications in lighting, display, and biosensing.

Acknowledgment. This work is supported by the National Nature Science Foundation (Grant Nos. 50973117, 21074139, 20904061, 50625312, 50671003, U0634004, and 20721061), and the 973 Program (2007CB936403, 2009CB930404, 2011CB932303 and 2011CB808400). The Chinese Academy of Sciences (No. KJCX-2-YW-M11) is gratefully acknowledged.

Supporting Information Available: SEM images of SiC inverse opal PCs obtained at varying calcination temperatures, reflectance spectra of SiC inverse opal PCs after being immersed in various solvents, hardness, and modulus curves of SiC PCs at varying fabrication temperatures. Photoluminescence enhancement of SiC PCs wih different stopbands. This material is available free of charge via the Internet at http://pubs.acs.org.

References and Notes

(1) Vukusic, P.; Hooper, I. *Science* **2005**, *310*, 1151.

(2) (a) Song, B. S.; Noda, S.; Asano, T.; Akahane, Y. *Nat. Mater.* **2005**, *4*, 207–210. (b) Lee, P. T.; Lu, T. W.; Fan, J. H.; Tsai, F. M. *Appl. Phys. Lett.* **2007**, *90*, 151125.

(3) (a) Lodahl, P.; van Driel, A. F.; Nikolaev, I. S.; Irman, A.; Overgaag, K.; Vanmaekelbergh, D. L.; Vos, W. L. *Nature* **2004**, *430*, 654–657. (b) Arsenault, A. C.; Clark, T. J.; von Freymann, G.; Cademartiri, L.; Sapienza, R.; Bertolotti, J.; Vekris, E.; Wong, S.; Kitaev, V.; Manners, I.; Wang, R. Z.; John, S.; Wiersma, D.; Ozin, G. A. *Nat. Mater.* **2006**, *5*, 179–184. (c) Chen, J. I. L.; von Freymann, G.; Choi, S. Y.; Kitaev, V.; Ozin, G. A. *J. Mater. Chem.* **2008**, *18*, 369–373. (d) Li, M. Z.; He, F.; Liao, Q.; Liu, J.; Xu, L.; Jiang, L.; Song, Y. L.; Wang, S.; Zhu, D. B. *Angew. Chem., Int. Ed.* **2008**, *47*, 7258–7262. (e) Li, H.; Wang, J. X.; Lin, H.; Xu, L.; Xu, W.; Wang, R. M.; Song, Y. L.; Zhu, D. B. *Adv. Mater.* **2010**, *22*, 1237–1241.

(4) Blanco, A.; Chomski, E.; Grabtchak, S.; Ibisate, M.; John, S.; Leonard, S. W.; Lopez, C.; Meseguer, F.; Míguez, H.; Mondia, J. P.; Ozin, G. A.; Toader, O.; van Driel, H. M. *Nature* **2000**, *405*, 437–440.

(5) (a) Zakhidov, A. A.; Baughman, R. H.; Iqbal, Z.; Cui, C. X.; Khayrullin, I.; Dantas, S. O.; Marti, I.; Ralchenko, V. G. *Science* **1998**, *282*, 897–901. (b) Li, H. L.; Chang, L. X.; Wang, J. X.; Yang, L. M.; Song, Y. L. *J. Mater. Chem.* **2008**, *18*, 5098–5103.

(6) Jiang, P.; Cizeron, J.; Bertone, J. F.; Colvin, V. L. *J. Am. Chem. Soc.* **1999**, *121*, 7957–7958.

(7) (a) Wijnhoven, J. E. G. J.; Vos, W. L. *Science* **1998**, *281*, 802–804. (b) Juarez, B. H.; Garcia, P. D.; Golmayo, D.; Blanco, A.; Lopez, C. *Adv. Mater.* **2005**, *17*, 2761–2765. (c) Scott, R. W. J.; Yang, S. M.; Chabanis, G.; Coombs, N.; Williams, D. E.; Ozin, G. A. *Adv. Mater.* **2001**, *13*, 1468–1472. (d) Waterhouse, G. I. N.; Metson, J. B.; Idriss, H.; Waterhouse, D. X. S. *Chem. Mater.* **2008**, *20*, 1183–1190.

(8) (a) Deutsch, M.; Vlasov, Y. A.; Norris, D. J. *Adv. Mater.* **2000**, *12*, 1176–1179. (b) Míguez, H.; Meseguer, F.; López, C.; Tejeira, F. L.; Dehesa, J. S. *Adv. Mater.* **2001**, *13*, 393. (c) Park, S. H.; Xia, Y. *Adv. Mater.* **1998**, *10*, 1045–1048. (d) Takeoka, Y.; Watanabe, M. *Adv. Mater.* **2003**, *15*, 199–201. (e) Matsubara, K.; Watanabe, M.; Takeoka, Y. *Angew. Chem., Int. Ed.* **2007**, *46*, 1688–1692.

(9) Yan, H. W.; Blanford, C. F.; Holland, B. T.; Smyrl, W. H.; Stein, A. *Chem. Mater.* **2000**, *12*, 1134–1141.

(10) (a) Ishikawa, T.; Kajii, S.; Matsunaga, K.; Hogami, T.; Kohtoku, Y.; Nagasawa, T. *Science* **1998**, *282*, 1295–1297. (b) Casady, J. B.; Johnson, R. W. *Solid-State Electron.* **1996**, *39*, 1409–1422.

(11) (a) Shi, Y. F.; Meng, Y.; Chen, D. H.; Cheng, S. J.; Chen, P.; Yang, H. F.; Wan, Y.; Zhao, D. Y. *Adv. Funct. Mater.* **2006**, *16*, 561–567. (b) Shi, Y. F.; Zhang, F.; Hu, Y. S.; Sun, X. H.; Zhang, Y. C.; Lee, H. I.; Chen, L. Q.; Stucky, G. D. *J. Am. Chem. Soc.* **2010**, *132*, 5552–5553. (c) Sung, I. K.; Yoon, S. B.; Yu, J. S.; Kim, D. P. *Chem. Commun.* **2002**, *14*, 1480–1481. (d) Wang, H.; Li, X. D.; Yu, J. S.; Kim, D. P. *J. Mater. Chem.* **2004**, *14*, 1383–1386. (e) Sung, I. K.; Christian; Mitchell, M.; Kim, D. P.; Kenis, P. J. A. *Adv. Funct. Mater.* **2005**, *15*, 1336–1342. (f) Christian; Mitchell, M.; Kenis, P. J. A. *Lab Chip* **2006**, *6*, 1328–1337.

(12) Ye, L; Han, W. J.; Zhang, R. L.; Hu, J. D.; Zhao, T. *J. Appl. Polym. Sci.* **2008**, *110*, 4064–4070.

(13) (a) Wang, J. X.; Wen, Y. Q.; Ge, H. L.; Sun, Z. W.; Zheng, Y. M.; Song, Y. L.; Jiang, L. *Macromol. Chem. Phys.* **2006**, *207*, 596–604. (b) Cui, L. Y.; Li, Y. F.; Wang, J. X.; Tian, E. T.; Zhang, X. Y.; Zhang, Y. Z.; Song, Y. L.; Jiang, L. *J. Mater. Chem.* **2009**, *19*, 5499–5502. (c) Cui, L. Y.; Zhang, Y. Z.; Wang, J. X.; Ren, Y. B.; Song, Y. L.; Jiang, L. *Macromol. Rapid Commun.* **2009**, *30*, 598–603.

(14) Calvo, M. E.; Sobrado, O. S.; Lozano, G.; Miguez, H. *J. Mater. Chem.* **2009**, *19*, 3144–3148.

(15) Kanai, T.; Sawada, T. *Langmuir* **2009**, *25*, 13315–13317.

(16) Hartman, J. S.; Richardon, M. F.; Sherriff, B. L.; Winsborrow, B. G. *J. Am. Chem. Soc.* **1987**, *109*, 6059–6067.

(17) Pol, V. G.; Pol, S. V.; Gedanken, A. *Chem. Mater.* **2005**, *17*, 1797–1802.

(18) Laine, R. M.; Babonneau, F. *Chem. Mater.* **1993**, *5*, 260–279.

(19) Bertone, J. F.; Jiang, P.; Hwang, K. S.; Mittleman, D. M.; Colvin, V. L. *Phys. Rev. Lett.* **1999**, *83*, 300–303.

(20) von Freymann, G.; John, S.; Dobrick, M. S.; Vekris, E.; Tetreault, N.; Wong, S.; Kitaev, V.; Ozin, G. A. *Appl. Phys. Lett.* **2004**, *84*, 224–226.

(21) (a) Blanford, C. F.; Schroden, R. C.; Al-Daous, M.; Stein, A. *Adv. Mater.* **2001**, *13*, 26–29. (b) Li, H. L.; Wang, J. X.; Yang, L. M.; Song, Y. L. *Adv. Funct. Mater.* **2008**, *18*, 3258–3264.

(22) (a) Miguez, H.; Tetreault, N.; Hatton, B.; Yang, S. M.; Perovic, D.; Ozin, G. A. *Chem. Commun.* **2002**, *22*, 2736–2737. (b) Tian, E. T.; Cui, L. Y.; Wang, J. X.; Song, Y. L.; Jiang, L. *Macromol. Rapid Commun.* **2009**, *30*, 509–514.

(23) (a) Wang, J. X.; Hu, J. P.; Wen, Y. Q.; Song, Y. L.; Jiang, L. *Chem. Mater.* **2006**, *18*, 4984–4986. (b) Xu, L.; Wang, J. X.; Song, Y. L.; Jiang, L. *Chem. Mater.* **2008**, *20*, 3554–3556.

(24) (a) Gu, Z.-Z.; Uetsuka, H.; Takahashi, K.; Nakajima, R.; Onishi, H.; Fujishima, A.; Sato, O. *Angew. Chem., Int. Ed.* **2003**, *42*, 894–897. (b) Sato, O.; Kubo, S.; Gu, Z.-Z. *Acc. Chem. Res.* **2009**, *42*, 1–10. (c) Gu, Z.-Z.; Fujishima, A.; Sato, O. *Appl. Phys. Lett.* **2004**, *85*, 5067–5069.

(25) (a) Matsumoto, T.; Takahashi, J.; Tamaki, T.; Futagi, T.; Mimura, H.; Kanemitsu, Y. *Appl. Phys. Lett.* **1994**, *64*, 226–228. (b) Chang, S. S.; Sakai, A. *Mater. Lett.* **2004**, *58*, 1212–1217.

(26) (a) Bechger, L.; Lodahl, P.; Vos, W. L. *J. Phys. Chem. B* **2005**, *109*, 9980–9988. (b) Jin, F.; Song, Y.; Dong, X.; Chen, W.; Duan, X. *Appl. Phys. Lett.* **2007**, *91*, 031109. (c) Ganesh, N.; Zhang, W.; Mathias, P. C.; Chow, E.; Soares, J. A. N. T.; Malyarchuk, V.; Smith, A. D.; Cunningham, B. T. *Nat. Nanotechnol.* **2007**, *2*, 515–520. (d) Chen, J. I. L.; Freymann, G. V.; Choi, S. Y.; Kitaev, V.; Ozin, G. A. *Adv. Mater.* **2006**, *18*, 1915–1919. (e) Maskaly, G. R.; Petruska, M. A.; Nanda, J.; Bezel, I. V.; Schaller, R. D.; Htoon, H.; Pietryga, J. M.; Klimov, V. I. *Adv. Mater.* **2006**, *18*, 343–347. (f) Liu, J.; Li, M. Z.; Wang, J. X.; Song, Y. L.; Jiang, L.; Murakami, T.; Fujishima, A. *Environ. Sci. Technol.* **2009**, *43*, 9425–9431.

(27) Shim, H. W.; Kim, K. C.; Seo, Y. H.; Nahm, K. S.; Suh, E. K.; Lee, H. J. *Appl. Phys. Lett.* **1997**, *70*, 1757–1759.

(28) Blum, C.; Mosk, A. P.; Nikolaev, I. S.; Subramaniam, V.; Vos, W. L. *Small* **2008**, *4*, 492–496.

JP108928G